

Compositional Screening of the Pb–Bi–Mo–O System. Spontaneous Formation of a Composite of *p*-PbMoO₄ and *n*-Bi₂O₃ with Improved Photoelectrochemical Efficiency and Stability

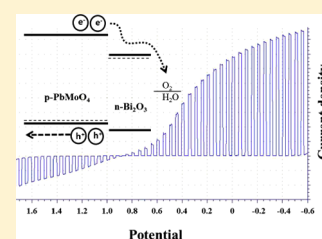
Ki Min Nam, Hyun S. Park, Heung Chan Lee, Benjamin H. Meekins, Kevin C. Leonard, and Allen J. Bard*

Center for Electrochemistry, Department of Chemistry and Biochemistry, The University of Texas at Austin, Austin, Texas 78712, United States

S Supporting Information

ABSTRACT: Scanning electrochemical microscopy (SECM) was used to identify more efficient p-type photocatalysts for H⁺ reduction in the Pb–Bi–Mo trimetal oxide system. An atomic ratio of (1:1:1) between Pb, Bi, and Mo showed higher photocurrent than other spots in screening experiments. The crystal structure of Pb–Bi–Mo oxide was studied by X-ray diffraction, indicating that a composite of *p*-PbMoO₄ and *n*-Bi₂O₃ coexisted as a heterostructure. Photoelectrochemical performance of the *p*-PbMoO₄/*n*-Bi₂O₃ composite electrode showed enhanced stability for the H⁺ and O₂ reduction reactions. We propose a reaction mechanism to explain this stabilization of a p-type semiconductor.

SECTION: Spectroscopy, Photochemistry, and Excited States



Previous work with scanning electrochemical microscopy (SECM) in the study of photocatalysts has shown that rapid synthesis and screening of arrays is useful in discovering single-phase materials as photocatalysts.¹ That concept is extended here to materials with two different phases and the investigation of the photoelectrochemical (PEC) behavior of composites. PEC water splitting using a metal oxide semiconductor is a promising method to produce hydrogen. Since the first suggestion of this concept,² much attention has been paid to semiconductor materials that could be used as photoelectrodes.^{3,4} The most critical issues in water splitting are the development of a photoelectrode with high efficiency and long-term stability in an aqueous environment. In principle, p-type semiconductors should be useful as photocathodes (for the reduction of H⁺ to H₂) in a PEC cell.⁵ Although high photocurrents have been attained with some photocathode materials, their low photovoltages and poor stabilities are critical problems.⁶ Most p-type semiconductor electrodes studied to date are generally unstable when used as photocathodes for proton reduction in an aqueous environment. This has been explained by a thermodynamic argument,^{7,8} that is, that the conduction band potential is more negative than that of the reduction potential of the metal ion in the lattice, leading to reductive decomposition of the semiconductor surface and loss of photoactivity.

Single semiconductor materials typically cannot satisfy the requirements of having suitable band gap energies for efficient solar absorption and band edges aligned for both H₂ and O₂ evolution reactions. Compared to single-component semiconductors, a composite heterojunction of two semiconductors has been studied as an attractive method to develop high-efficiency materials by absorbing different regions of the solar

spectrum.⁹ In addition, by forming a junction structure, it can promote efficient electron–hole separation and reduce recombination.

SECM Screening of Pb–Bi–Mo–O Arrays. To investigate the effect of photocatalyst compositions, Pb–Bi–Mo oxide arrays were prepared on a fluorine-doped tin oxide (FTO) substrate by automated dropwise dispensing¹ of different ratios of solutions of a 20 mM Pb precursor (Pb(NO₃)₂) as the first component, a 20 mM Bi precursor (Bi(NO₃)₃·5H₂O) as the second, and a 20 mM Mo precursor ((NH₄)₆Mo₇O₂₄·4H₂O) as the third. After completing the dispensing, the arrays were annealed in air at 600 °C for 3 h, and then, the arrays were screened with a scanning optical fiber connected to a Xe lamp. The detailed method is provided in the Supporting Information.¹ Figure 1a shows the dispensed pattern of the triangular array. The top corner is PbO. The bottom left and right corners are Bi₂O₃ and MoO₃, respectively. The first, left column was composed of only Pb–Bi oxides, and the bottom row contained only Bi–Mo oxides. Figure 1b shows the photocurrent image of the array under UV–visible light irradiation. The applied potential was 0 V versus Ag/AgCl in 0.1 M Na₂SO₄ and 0.2 M sodium phosphate buffer (pH 7). Spots A and B had Pb/Bi/Mo oxide atomic ratios of 3:3:3 and 4:2:3, respectively. They show a higher cathodic photocurrent than the other spots under UV–vis light irradiation. This photocurrent is nearly twice as high as that of Pb–Mo oxide spots in the same array (Figure 1b).

Received: June 28, 2013

Accepted: July 26, 2013

Published: July 26, 2013

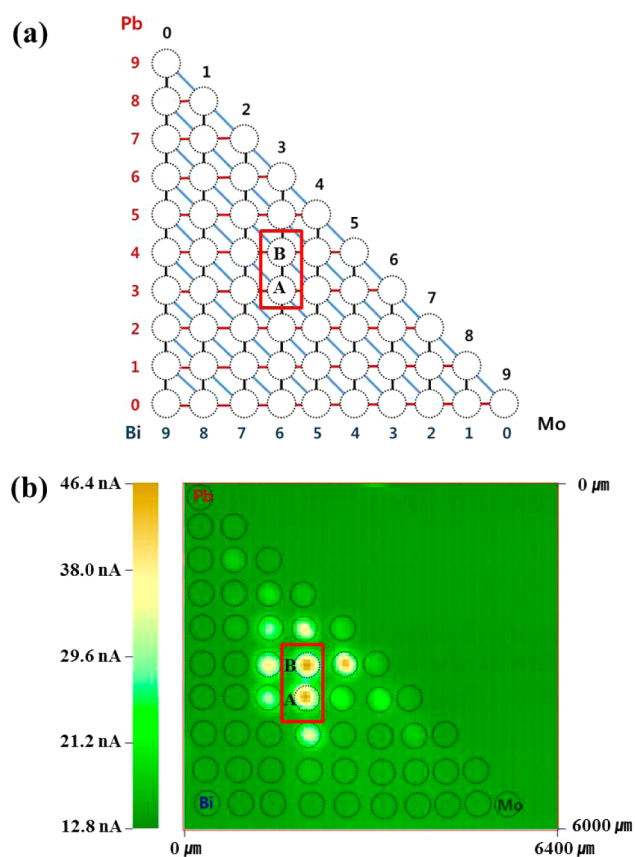


Figure 1. (a) Dispensed pattern of photocatalyst arrays with three components. The top corner is pure Pb, the bottom left corner is Bi, and the bottom right corner is Mo. Spots A and B represent Pb–Bi–Mo at 3:3:3 and 4:2:3 atomic ratios, respectively. (b) SECM image of a Pb–Bi–Mo oxide photocatalyst at an applied potential of 0 V versus Ag/AgCl in 0.1 M Na₂SO₄ with 0.2 M phosphate buffer solution (pH 7).

PEC at Macroelectrodes. To confirm the improved photoactivity of Pb–Bi–Mo oxide, thin film electrodes were prepared by drop casting the solutions on a FTO substrate. The atomic ratio between Pb, Bi, and Mo was 1:1:1 according to the results from SECM experiments. The scanning electron microscopy (SEM) image showed a porous morphology with small grain sizes below 150 nm (Figure S1 in the Supporting Information). The XRD pattern of the Pb–Bi–Mo oxide thin film (Figure 2) matched well with patterns of a composite of PbMoO₄¹⁰ and Bi₂O₃¹¹ on the FTO substrate. The crystallite sizes were ~55 (PbMoO₄) and ~30 nm (Bi₂O₃) as determined by the Scherrer equation.¹² In comparison with their standard PbMoO₄, the peaks were shifted slightly toward higher angles (Figure S2a, Supporting Information), while the Bi₂O₃ peaks were shifted toward lower angles (Figure S2b, Supporting Information). These XRD data suggest that the PbMoO₄ lattice is slightly compressed and the Bi₂O₃ lattice is expanded in a PbMoO₄/Bi₂O₃ heterostructure. This result can be interpreted as an effect of the lattice mismatch at the junction of the two materials.¹³

The PEC performance of the Bi₂O₃, PbMoO₄, and PbMoO₄/Bi₂O₃ composite electrode was studied using linear sweep voltammetry (LSV) in 0.1 M Na₂SO₄ (pH 7, 0.2 M sodium phosphates buffered). Previous studies of PbMoO₄ as powders have demonstrated H₂ and O₂ production with sacrificial reagents;¹⁴ however, the nature of the powder (p-type or n-

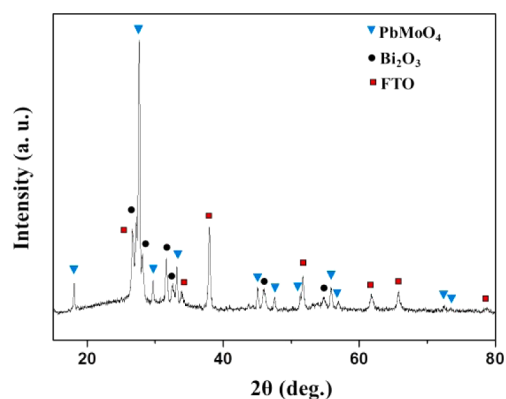


Figure 2. XRD patterns of a Pb–Bi–Mo (1:1:1) oxide thin film annealed at 600 °C for 3 h in air atmosphere. Red square peaks are from the FTO substrate.

type) was not determined. Bi₂O₃ has been reported to be an amphoteric semiconductor with n- and p-type behavior depending on the crystal structure.¹⁵ In the case of n-type Bi₂O₃, the band gap is 2.75 eV with a conduction band edge of +0.11 V (versus NHE).¹⁶

The PEC performance of as-prepared Bi₂O₃ shows n-type photoresponse, and PbMoO₄ shows p-type response (Supporting Information Figure S3). The *p*-PbMoO₄/*n*-Bi₂O₃ composite electrode shows both anodic and cathodic photocurrents under UV–vis irradiation depending on the potential (Figure 3a). The cathodic photocurrent onset potential in a pH 7 solution is ~0.8 V versus Ag/AgCl, indicating that the *p*-PbMoO₄ composite electrode is quite suitable for generating H₂ from water, even without an electrocatalyst like Pt.

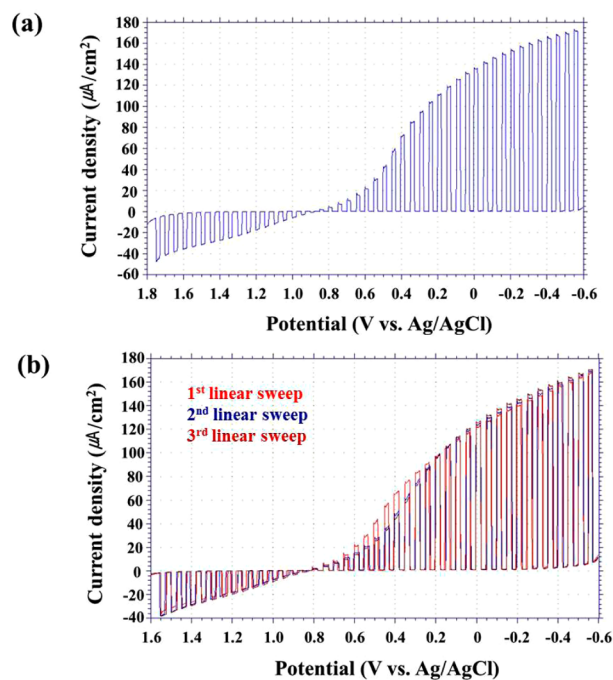


Figure 3. (a) LSV of a *p*-PbMoO₄/*n*-Bi₂O₃ composite electrode in deaerated 0.1 M Na₂SO₄ and 0.2 M sodium phosphate buffer (pH 7, Ar bubbling) under UV–vis irradiation and (b) LSVs of the same sample to study the stability of the prepared film. Scan rate: 15 mV/s. Light intensity: 100 mW/cm².

Stability and IPCE. When LSVs of the same composite sample were repeated three times under the same conditions, no changes were seen (Figure 3b). This indicates that the $p\text{-PbMoO}_4/n\text{-Bi}_2\text{O}_3$ composite suppresses the decomposition of the electrode itself compared to $p\text{-PbMoO}_4$ alone (Figure S3a, Supporting Information). To assess the stability of the $p\text{-PbMoO}_4/n\text{-Bi}_2\text{O}_3$ electrode over time, chronoamperometry was carried out at 0 V versus Ag/AgCl under full-spectrum illumination in an air atmosphere (Figure 4a). The $p\text{-PbMoO}_4/$

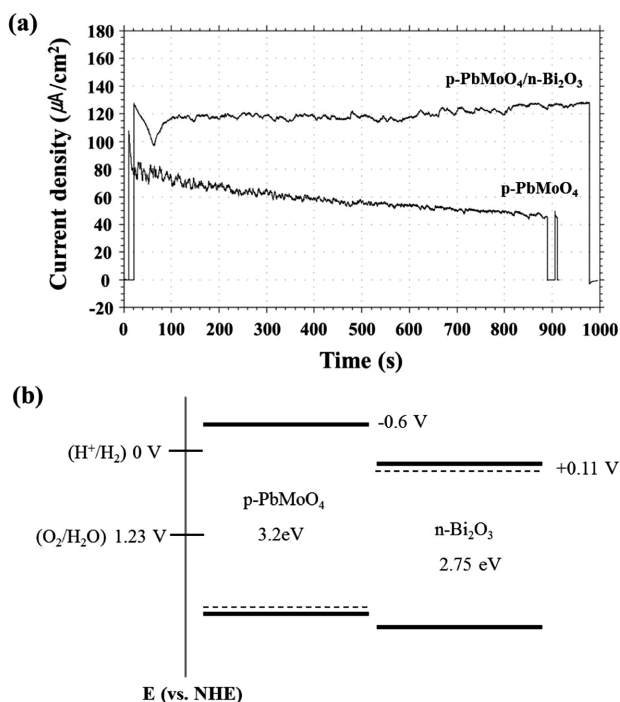


Figure 4. (a) Current–time response curve of the $p\text{-PbMoO}_4/n\text{-Bi}_2\text{O}_3$ composite electrode at an applied potential of 0 V versus Ag/AgCl in 0.1 M Na_2SO_4 with a 0.2 M phosphate buffer solution (pH 7, air bubbling) under UV–vis light irradiation. (b) Energy band diagram for the $p\text{-PbMoO}_4/n\text{-Bi}_2\text{O}_3$ heterostructure.

$n\text{-Bi}_2\text{O}_3$ electrode showed high photoelectrochemical stability when O_2 was present as the electron acceptor, while the photocurrent of $p\text{-PbMoO}_4$ alone under the same conditions decayed rapidly, dropping by $\sim 50\%$ over 15 min, indicating instability of $p\text{-PbMoO}_4$ (Figure 4a). Photocathodic instability of metal oxides is typically attributed to the preferential reduction of the lattice metal cations.^{3,17}

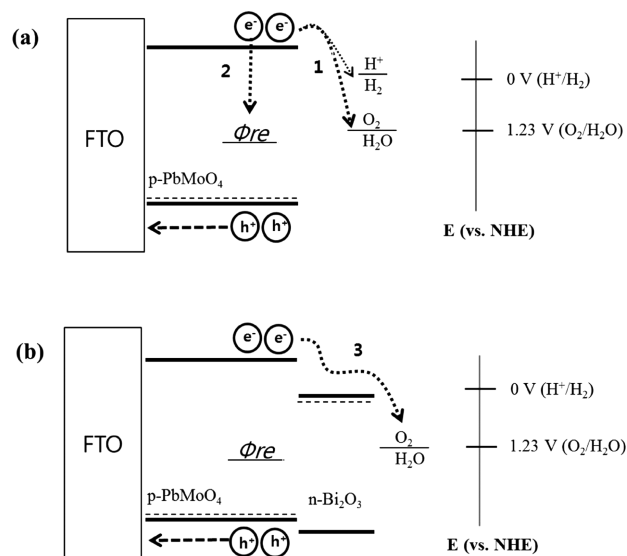
The UV–visible absorption spectrum of the $p\text{-PbMoO}_4/n\text{-Bi}_2\text{O}_3$ composite electrode is shown in Figure S4 in the Supporting Information. The incident photon to electron conversion efficiencies (IPCEs) plot at 0 V versus Ag/AgCl is also presented in Supporting Information Figure S4. The calculated IPCE for proton reduction at pH 7 reached $\sim 28\%$ at 340 nm and decreased with increasing wavelength and reached zero at ~ 400 nm. The band gap of PbMoO_4 is ~ 3.2 eV, in agreement with a previous study.¹⁴

For the reduction of H^+ to H_2 with the $p\text{-PbMoO}_4/n\text{-Bi}_2\text{O}_3$ electrode, chronoamperometry was carried out at 0 V versus Ag/AgCl under full spectrum irradiation (pH 7, argon). After the chronoamperometry, the evolved H_2 gas was gathered using a gastight syringe and analyzed using gas chromatography–mass spectroscopy (Supporting Information Figure S5). Although the $p\text{-PbMoO}_4/n\text{-Bi}_2\text{O}_3$ shows instability and a very

low H_2 conversion ratio under argon, this experiment clearly confirms that photogenerated electrons in the conduction band of $p\text{-PbMoO}_4$ can be used for H_2 evolution (Figure 4b).

Proposed Mechanism. There are two possible explanations for the improved photocurrent and stabilization, composite effects or doping of the $p\text{-PbMoO}_4$ and $n\text{-Bi}_2\text{O}_3$. For example, the Bi_2O_3 may have been doped with Mo or Pb, with Mo providing a sufficiently negative reduction potential for H_2 evolution. Alternatively, the enhancement of the $p\text{-PbMoO}_4$ could result from Bi doping. However, we have found that $p\text{-PbMoO}_4$ doped with 4% Bi and Bi_2O_3 doped with small amounts of Pb or Mo do not show any improvement in photoactivity or stability. Thus, we ascribe both the enhancement and stabilization to composite effects. The mechanism of photocatalytic H^+ or O_2 reduction at $p\text{-PbMoO}_4$ and the $p\text{-PbMoO}_4/n\text{-Bi}_2\text{O}_3$ composite electrode is shown in Scheme 1. It is

Scheme 1. Energy Band Diagram for (a) $p\text{-PbMoO}_4$ and (b) the $p\text{-PbMoO}_4/n\text{-Bi}_2\text{O}_3$ Heterostructure^a



^aThe dashed line is the Fermi level. Pathway (1), O_2 reduction at the $p\text{-PbMoO}_4$ surface, (2) semiconductor (PbMoO_4) reduction, (3) O_2 reduction at the $n\text{-Bi}_2\text{O}_3$ surface. The Φ_{re} is the thermodynamic reduction potentials of the semiconductor (PbMoO_4).

unlikely that a p–n junction will form under the conditions of composite synthesis; therefore, we represent the bands without Fermi level equilibration. The $p\text{-PbMoO}_4$ absorbs photons to generate excited electrons that can reduce H^+ or O_2 (pathway 1 in Scheme 1a). In many cases, p-type photocatalysts are unstable because the electrode material reacts with the photogenerated electrons (pathway 2 in Scheme 1a), depending on the thermodynamic reduction potentials of the semiconductor, for example, PbMoO_4 (Φ_{re}),^{7,17} and this material shows instability under irradiation (Figure 4a). When the p-semiconductor ($p\text{-PbMoO}_4$) and n-semiconductor ($n\text{-Bi}_2\text{O}_3$) materials are in contact, we propose that they form a spontaneous composite structure (Scheme 1b). In the photogenerated electron/hole pairs, photoexcited electrons migrate to $n\text{-Bi}_2\text{O}_3$ at the p–n interface, which can reduce O_2 (pathway 3 in Scheme 1b). This electron transfer to the $n\text{-Bi}_2\text{O}_3$ suppresses the decomposition of the $p\text{-PbMoO}_4$ and also reduces recombination at the surface compared to $p\text{-PbMoO}_4$ alone.

The composite electrode showed a large initial drop during chronoamperometry in argon (Supporting Information Figure S6) due to the decomposition of the electrode itself because the conduction band of Bi_2O_3 is too positive to evolve hydrogen. When oxygen was reintroduced after initially irradiating the composite electrode under argon, the photocurrent slowly recovered and stabilized after 5 min (Supporting Information Figure S6). This indicated that photogenerated holes could reoxidize the reduced $p\text{-PbMoO}_4$ (pathway 4 in Figure S6, Supporting Information), counteracting the photoreduction (Φ_{re}) and restoring the p -type semiconductor.

In summary, SECM was used to identify more efficient p -type photocatalysts for H^+ and O_2 reduction in the Pb-Bi-Mo trimetal oxide system. An atomic ratio of (1:1:1) between Pb , Bi , and Mo showed higher photocurrent than other spots from screening experiments. The Pb-Bi-Mo oxide was studied using X-ray diffraction, indicating that a composite of $p\text{-PbMoO}_4$ and $n\text{-Bi}_2\text{O}_3$ coexists as a heterostructure electrode. The enhanced stability for O_2 reduction with the $p\text{-PbMoO}_4/n\text{-Bi}_2\text{O}_3$ composite is ascribed to electron transfer to the $n\text{-Bi}_2\text{O}_3$. The spontaneous formation of composite structures of oxide semiconductors that show improved PEC performance represents another approach to photocatalyst optimization.

■ ASSOCIATED CONTENT

■ Supporting Information

Details of synthetic procedures, XRD pattern, SEM image, and LSV results of the $p\text{-PbMoO}_4/n\text{-Bi}_2\text{O}_3$ composite electrode. This material is available free of charge via the Internet at <http://pubs.acs.org>.

■ AUTHOR INFORMATION

■ Corresponding Author

*E-mail: ajbard@mail.utexas.edu.

■ Notes

The authors declare no competing financial interest.

■ ACKNOWLEDGMENTS

We acknowledge the Division of Chemical Sciences, Geosciences, and Biosciences Office of Basic Energy Sciences of the U.S. Department of Energy-SISGR (DE-FG02-09ER16119) and the Robert A. Welch Foundation (F-0021) for financial support of this project.

■ REFERENCES

- (1) Lee, J.; Ye, H.; Pan, S.; Bard, A. J. Screening of Photocatalysts by Scanning Electrochemical Microscopy. *Anal. Chem.* **2008**, *80*, 7445–7450.
- (2) Fujishima, A.; Honda, K. Electrochemical Photolysis of Water at a Semiconductor Electrode. *Nature* **1972**, *238*, 37–38.
- (3) Bard, A. J.; Fox, M. A. Artificial Photosynthesis: Solar Splitting of Water to Hydrogen and Oxygen. *Acc. Chem. Res.* **1995**, *28*, 141–145.
- (4) Kudo, A.; Miseki, Y. Heterogeneous Photocatalyst Materials for Water Splitting. *Chem. Soc. Rev.* **2009**, *38*, 253–278.
- (5) Bard, A. J. Photoelectrochemistry. *Science* **1980**, *207*, 139–144.
- (6) Paracchino, A.; Laporte, V.; Sivula, K.; Gratzel, M.; Thimsen, E. Highly Active Oxide Photocathode for Photoelectrochemical Water Reduction. *Nat. Mater.* **2011**, *10*, 456–461.
- (7) Bard, A. J.; Wrighton, M. S. Thermodynamic Potential for the Anodic Dissolution of n -Type Semiconductors: A Crucial Factor Controlling Durability and Efficiency in Photoelectrochemical Cells and an Important Criterion in the Selection of New Electrode/Electrolyte Systems. *J. Electrochem. Soc.* **1977**, *124*, 1706–1710.

- (8) Gerischer, H. Electrochemical Photo and Solar Cells Principles and Some Experiments. *J. Electroanal. Chem. Interfacial Electrochem.* **1975**, *58*, 263–274.

- (9) Nozik, A. J. Photoelectrochemistry: Applications to Solar Energy Conversion. *Annu. Rev. Phys. Chem.* **1978**, *29*, 189–222.

- (10) Shen, M.; Zhang, Q.; Chen, H.; Peng, T. Hydrothermal Fabrication of PbMoO_4 Microcrystals with Exposed (001) Facets and Its Enhanced Photocatalytic Properties. *CrystEngComm* **2011**, *13*, 2785–2791.

- (11) Fan, H. T.; Pan, S. S.; Teng, X. M.; Ye, C.; Li, G. H. Structure and Thermal Stability of $\delta\text{-Bi}_2\text{O}_3$ Thin Films Deposited by Reactive Sputtering. *J. Phys. D: Appl. Phys.* **2006**, *39*, 1939–1943.

- (12) Cullity, B. D. *Elements of X-Ray Diffraction*; Addison-Wesley: Reading, MA, 1978.

- (13) Wu, H.; Chen, O.; Zhuang, J.; Lynch, J.; Lamontagne, D.; Nagaoka, Y.; Cao, Y. C. Formation of Heterodimer Nanocrystals: $\text{UO}_2/\text{In}_2\text{O}_3$ and $\text{FePt}/\text{In}_2\text{O}_3$. *J. Am. Chem. Soc.* **2011**, *133*, 14327–14337.

- (14) Kudo, A.; Steinberg, M.; Bard, A. J.; Campion, A.; Fox, M. A.; Mallouk, T. E.; Webber, S. E.; White, J. M. Photoactivity of Ternary Lead-Group IVB Oxides for Hydrogen and Oxygen Evolution. *Catal. Lett.* **1990**, *5*, 61–66.

- (15) Hardee, K. L.; Bard, A. J. Semiconductor Electrodes X. Photoelectrochemical Behavior of Several Polycrystalline Metal Oxide Electrodes in Aqueous Solutions. *J. Electrochem. Soc.* **1977**, *124*, 215–224.

- (16) Lin, X.; Xing, J.; Wang, W.; Shan, Z.; Xu, F.; Huang, F. Photocatalytic Activities of Heterojunction Semiconductors $\text{Bi}_2\text{O}_3/\text{BaTiO}_3$: A Strategy for the Design of Efficient Combined Photocatalysts. *J. Phys. Chem. C* **2007**, *111*, 18288–18293.

- (17) Chen, S.; Wang, L.-W. Thermodynamic Oxidation and Reduction Potentials of Photocatalytic Semiconductors in Aqueous Solution. *Chem. Mater.* **2012**, *24*, 3559–3567.